



## Performance evaluation of two-stage spiral wound forward osmosis elements at various operation conditions

Sung-Ju Im<sup>a</sup>, Gyeong-Wan Go<sup>a</sup>, Sang-Hak Lee<sup>b</sup>, Gi-Ho Park<sup>c</sup>, Am Jang<sup>a,\*</sup>

<sup>a</sup>Graduate School of Water Resources, Sungkyunkwan University (SKKU), 2066, Seobu-ro, Jangan-gu, Suwon-si, Gyeonggi-do 16419, Korea, emails: [juim90@gmail.com](mailto:juim90@gmail.com) (S.-J. Im), [gogyewwan8329@gmail.com](mailto:gogyewwan8329@gmail.com) (G.-W. Go), Tel. +82 31 290 7535;

Fax: +82 31 290 7549; email: [amjang@skku.edu](mailto:amjang@skku.edu) (A. Jang)

<sup>b</sup>Huviswater Corporation, 425-100 (Moknae-dong) 90, Sandan-ro 83beon-gol, Danwon-Gu, Ansan-si, Gyeonggi-do, Korea, email: [leesh@huviswater.com](mailto:leesh@huviswater.com)

<sup>c</sup>Plant & Environment Research Team, DICT (Daewoo Institute of Construction Technology), 60, Songjuk, Jangan-gu, Suwon, Gyeonggi-do 440-210, Korea, email: [giho.park@daewooenc.com](mailto:giho.park@daewooenc.com)

Received 23 October 2015; Accepted 17 February 2016

---

### ABSTRACT

Forward osmosis (FO) is an emerging process in water industry for wastewater treatment, water reuse, and desalination. Although many lab-scale studies have been done, the data generated cannot be directly applied to a real pilot plant due to different membrane configuration and operating conditions. In this study, we evaluated commercial spiral wound forward osmosis (SWFO) elements in various operating conditions (draw solution concentration, flow rate, and element array type). First, we investigated the SWFO special structure (winding configuration of the draw flow path). Due to the structural characteristics of SWFO, the draw flow rate showed a high-pressure drop effect because of feed flow rate. Second, we studied the performance of different element array types. Both sides of flow rate change influenced the performance of pilot-scale SWFO by reducing concentration polarization and dilution effect. In addition, according to the type of SWFO element array, the flow rate had different role in water flux. We propose guidelines for the design and management of commercial FO processes to carry out element evaluation as directly applicable to pilot plant. This study can be used as an important reference for engineers in the FO process field.

*Keywords:* Forward osmosis; Pilot-scale; Spiral wound element; Flow rate; Water flux

---

### 1. Introduction

To overcome or attenuate global warming and water scarcity crises, enormous efforts and research

studies have been done to identify novel methods to purify wastewater or seawater at low cost with low energy consumption [1–3]. Membrane process such as reverse osmosis (RO), nanofiltration (NF), and ultrafiltration (UF) have emerged for water treatment, desalination, and water reuse because the area for

---

\*Corresponding author.

*Presented at 2015 Academic Workshop for Desalination Technology held in the Institute for Far Eastern Studies Seoul, Korea, 23 October 2015*

membrane process installation is compact. In addition, their removal efficiency is higher than traditional water treatment processes such as sand filtration or settling reservoir [2–4].

RO and NF are effective and commercially available technologies in the water industry [4,5]. However, pressure-driven membrane processes require expensive capital expenditures (CAPEX) and operating expenditures (OPEX) because they necessitate high hydraulic pressure to overcome the source osmotic pressure with resistance to foulants [2,6,7]. Forward osmosis (FO) is one membrane process driven by different mechanisms. In the FO process, water is transported through semi-permeable membrane from a low concentration solution (feed solution) to a high concentration solution (draw solution) creating a difference in osmotic pressure [8]. The basic FO mechanism has many advantages such as high water recovery, low operation pressure, less fouling tendency, and easy cleaning. For these reasons, FO is widely used in food, medical, and pharmaceutical industries except for water treatment [8–11]. In order to influence the water industry, FO must prove to surpass the current water purification processes. First, the FO membrane needs to have high water permeation with superior salt separation. Second, the FO process should reach similar theoretical value. Third, FO researchers need to find a suitable draw solution and fouling control for FO management. Fourth, the FO process needs to address problems such as concentration polarization (CP), cleaning methods, membrane lifetime, and reverse solute flux [6,12–14].

Many FO membrane and process studies have been conducted at lab-scale level using a flat sheet membrane coupon [10,15]. A few studies used a spiral-wound membrane, however, we still need further study at the pilot-scale [11,16–18]. Nevertheless, lab-scale FO test data cannot be directly applied to a real pilot plant for water purification. Thus, after commercialized FO element evaluation, it is preferable to progress to the next step to scale up the FO process.

For the evaluation of commercialized FO elements, the following need to be considered: (1) there are a few FO membrane manufacturers, such as Hydration Technology Innovations (HTI), Porifera, and Toray. (The HTI spiral wound forward osmosis (SWFO) element was used in this study); (2) spiral-wound and flat sheet elements have different configurations and flow path distance, meaning that different drops in pressure and permeate flux may develop depending on structural characteristics [15,19]. Therefore, we determined the spiral-wound structural characteristic of SWFO through a pilot-scale apparatus. In addition, we performed comparative studies to identify capacities of two types of

array (series and parallel) at various draw solution concentrations (25,000–70,000 ppm). We also examined the effect of flow rate change on FO performance. The aim of this study was to obtain directly applicable data for real pilot plant to provide basic information to scaling up the FO process.

## 2. Materials and methods

### 2.1. SWFO element and membrane

The commercially available SWFO element (HTI OsMem™ 2521 FO-CTA-MS-P-3H) was provided by HTI (Albany, USA) to evaluate SWFO performance. The SWFO element was made by wrapping one flat sheet membrane with embedded support. The membrane consisted of a cellulose triacetate (CTA) layer with an embedded polyester mesh for mechanical support. It is 50  $\mu\text{m}$  thick [13,20]. The effective membrane area is 0.5  $\text{m}^2$ . The length and width of the element was 0.52 and 0.48 m, respectively. The SWFO element has a standard diamond-type feed spacer with thickness of 1.1 mm and a 3H draw solution spacer 1.5 mm thick. The spacer enhanced the turbulence in flow. It can reduce the CP and the rate of mass transfer on the surface of membrane [15,17,21]. The SWFO element used in this study had a cross flow pattern.

The membrane active layer faced the feed solution while support layer later faced the draw solution (AL-facing-FS mode). According to its specification information, the element was capable of enduring a maximum operating temperature of 43°C with maximum side-port pressure of five bars. The maximum transmembrane pressure (side-port exit pressure minus end-port feed pressure) was 0.35 bar. The maximum end-port inlet and outlet pressures were one bar and 0.15 bar, respectively. The solution pH ranged from 3 to 8, with maximum NTU of 10. The maximum tolerable hydraulic pressure of the polyvinyl chloride (PVC) vessel was 15 bars.

The SWFO element is different from a RO vessel because FO has different mechanisms compared to RO [2,3]. As shown in Fig. 1, the SWFO element was housed in a pressure vessel (AXEON water technologies, CA) of PVC with four ports. Two ports were for inlet of feed and draw solution. The remaining two ports were for outlet of concentrated feed and diluted draw solution.

### 2.2. Pilot-scale spiral-wound forward osmosis design

Fig. 2a shows a schematic diagram of the FO–RO hybrid pilot system. Our pilot system is composed of

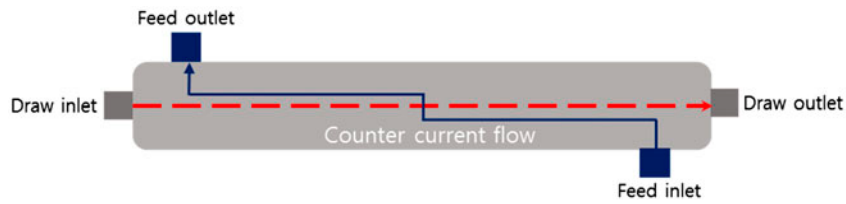


Fig. 1. SWFO PVC vessel with four ports.

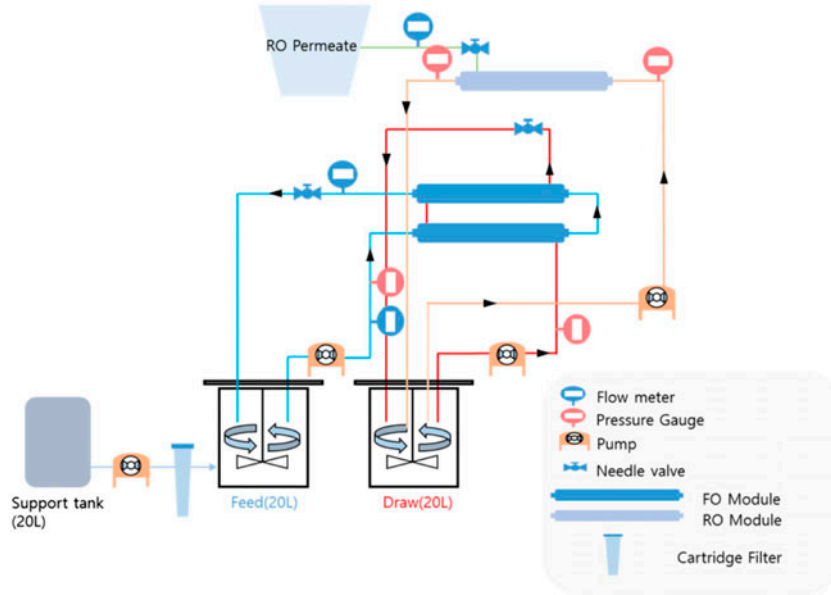


Fig. 2a. Schematic diagram of the FO-RO pilot system.

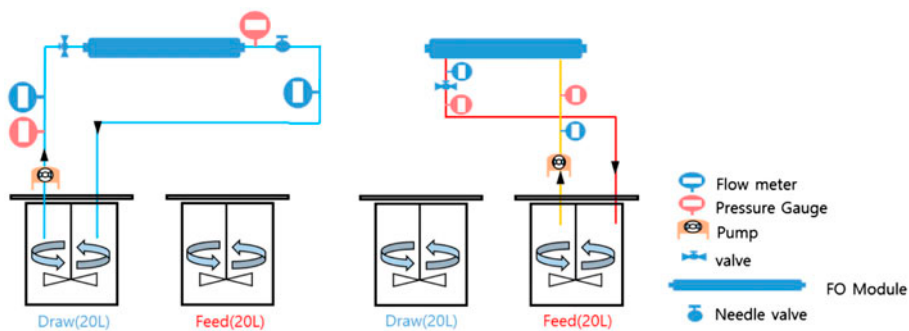


Fig. 2b. Schematic diagram of the one-stage SWFO element.

two SWFO elements and one SWRO element. In this study, we focused on the two SWFO elements system because the SWFO evaluation must precede the operation of the FO-RO hybrid system. SWFO elements were connected in series or in parallel, in two-stage or one-stage modes.

As seen in Fig. 2b, in the one-stage mode, both draw solution and feed solution flowed in each side inlet and flowed out through each side outlet. Both solutions were then fed back to each tank. In contrast, in the two-stage mode, the effluent of first FO element moved directly toward the second SWFO element as

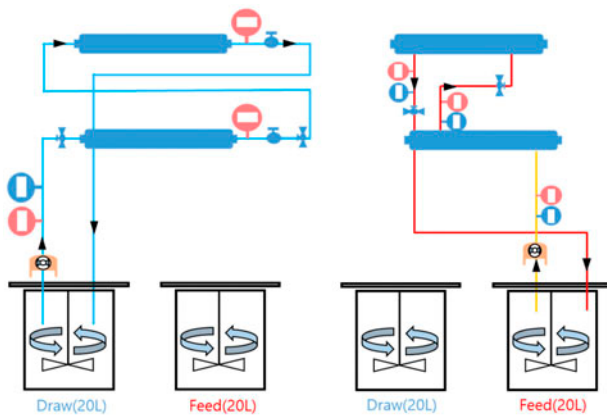


Fig. 2c. Schematic diagram of the two-stage SWFO element.

shown in Fig. 2c, meaning that the draw solution was diluted and the feed solution was concentrated one more time in the second stage of the two-stage mode. In the one-stage mode, only one osmotic dilution worked through the single SWFO element. Shortly after the operation, the retention time and dilution effect inside the element were different at each stage mode.

Pressure transmitters, conductivity meter (Orion 4 Star, Thermo Scientific, Albany, USA), flow meter (feed side), and mass cylinder (draw side) were installed to measure the pressure, conductivity, flow rate, and RSF, respectively. An electronic balance (Portable Bench, CAS, Korea) was installed under the feed and draw solution tanks to measure water flux. The flow rate and pressure were controlled with an inverter installed on both sides of the solutions. All data were recorded at four min intervals. An agitator was installed on both sides of the tanks to maintain the concentration in the tank. The tank volume was 20 L. The experiment was stopped when the volume of feed solution tank decreased below 50%. At the end of every experiment, physical cleaning was conducted to remove salt deposition onto the FO membrane surface.

### 2.3. Water flux, reverse salt flux (RSF), and recovery rate measurement

Eq. (1) was used to calculate water flux:

$$J_w = \frac{\text{Initial feed weight (kg)} - \text{Feed weight (kg)}}{\text{Test time (min)} \times 60 \text{ (min)} \div \text{Effective membrane area (m}^2\text{)}} \quad (1)$$

In Eq. (2), RSF was determined by measuring the conductivity meter installed inside the feed tank. RSF was converted to NaCl concentration using a pre-determined conductivity calibration curve vs. NaCl concentration.

$$J_s = \frac{C_t V_t - C_0 V_0}{A_t} \quad (2)$$

In the above equation, the  $C_0$  and  $C_t$  are the concentrations of NaCl in the feed tank at time (0) and certain time ( $t$ ), respectively; whereas  $V_0$  and  $V_t$  were the volume of feed tank at time (0) and at time ( $t$ ), respectively.

The recovery rate was calculated using the following Eq. (3) [9]:

$$\text{Recovery (\%)} = \frac{Q_{\text{Permeate}}}{Q_{\text{Feed}}} \quad (3)$$

where  $Q_{\text{feed}}$  and  $Q_{\text{permeate}}$  are the feed rate and permeate flow rate (LPM), respectively.

### 2.4. Test conditions of the SWFO element test

The SWFO element test was conducted under various operating conditions (Table 1) To analyze FO performance, the solution concentration and array type were changed under certain conditions. All tests were carried out at room temperature. DI water and NaCl solution (Samchun chemicals, Korea) were used as feed solution and draw solution, respectively.

## 3. Results and discussion

### 3.1. Performance of SWFO element compared to flat sheet FO membrane

Water flux and RSF of flat sheet FO membrane and SWFO membrane in AL-facing-FS mode (FO mode), as a function of draw solution, are shown in Fig. 3. The water flux and RSF increased logarithmically when the draw solution concentration was increased. This could be due to CP phenomenon, such as dilutive internal CP and concentrative external CP [10,22,23].

Interestingly, when the results in Fig. 3(a) and (b) were compared, water flux in the lab-scale test was

Table 1

Operating conditions and specification of the membrane used in the SWFO element of pilot experiments

Feed flow rate (LPM)	3.3–6.6
Draw flow rate (LPM)	0.35–0.55
Draw solution concentration (ppm)	25,000–70,000
Feed solution	DI water
Draw solution	NaCl solution
Array type	One stage (parallel array) Two stage (series array)
Operating temperature (°C)	21–23

twice higher than that in the SWFO element test. This may be explained by the following: first, no significant dilution effect occurred in membrane channel in the lab-scale test compared to that in the pilot-scale test because SWFO membrane had a long flow path for draw solution. In addition, the draw solution was consistently diluted along the pathway, thus losing driv-

ing force (osmotic pressure) [12]. Therefore, the dilution level of the draw solution in the lab-scale experiment was different from that in the pilot-scale test. To mitigate this phenomenon, we recommend that a counter-current flow path may be more efficient than co-current [12,24].

Second, The SWFO element membrane has a dead zone [24,25]. This is because the SWFO flow path inside of the draw solution has a winding structure. An illustration of the SWFO element is depicted in Fig. 4 [10]. In this illustration, a dead zone is formed in the edge of the draw flow path. Because of this dead zone, the membrane effective area decreased, thus decreasing the water flux. According to previous studies [6,10,15], an increased flow rate on both sides can play a positive role in the water flux due to reduced CP effect and the enhanced mass transfer coefficient. However, a spiral-wound membrane applied in real plant process, can not only form the dead zone, but also can have different dead zone

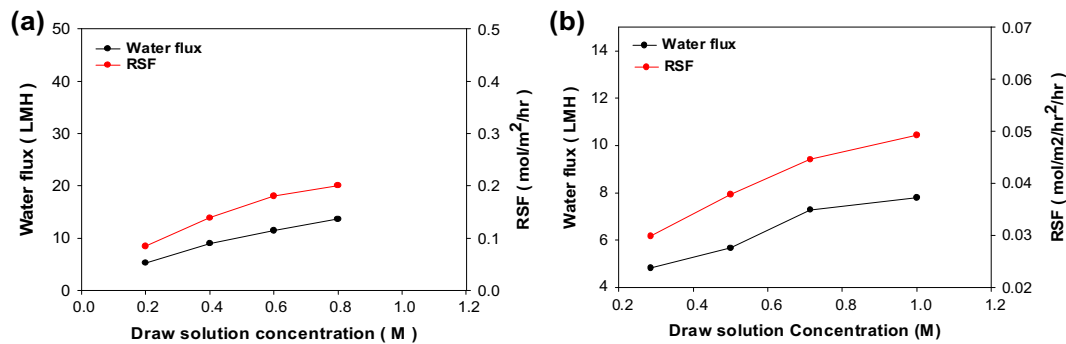


Fig. 3. Water flux and RSF comparison of two membranes with different shapes and sizes at varying draw solution concentrations: (a) Lab-scale flat sheet FO membrane test. The flow rate at both sides was 0.4 LPM at 25°C. The membrane area was 20.02 cm<sup>2</sup> and (b) The SWFO element test. The feed rate and draw flow rate were maintained constantly at 3.3 and 0.35 LPM, respectively. The membrane area was one m<sup>2</sup>.

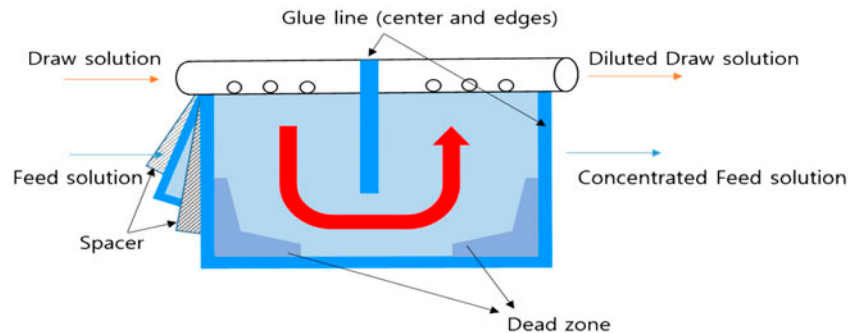


Fig. 4. An illustration of flow path and SWFO component element. Draw solution and feed solution flowed into the main pipe and space between membranes. Spacers were used both inside and outside the membrane [10,16].

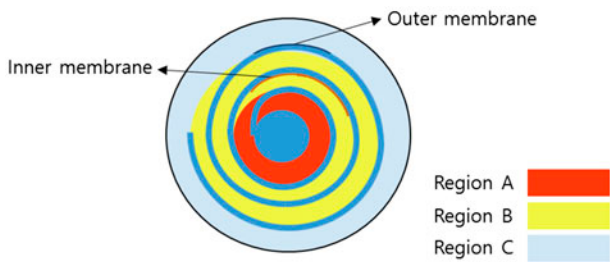


Fig. 5. Structure characteristics of Winding SWFO membrane.

shape if the flow rate changes. Therefore, different results between lab-scale and SWFO element test were found.

Third, the SWFO element had a different water flux distribution by membrane region because membranes were rolled-up around the main draw solution pipe with different effective membrane areas (Fig. 5). In the regions of A and C, only the inner or outer membrane had contact with the draw solution. However, in the region of B, both inner and outer membranes contacted the draw solution. According to previous studies, region B has lower water flux than region A and C. In other words, SWFO has heterogeneity in water flux by region. Therefore, the SWFO system showed poor performance compared to flat sheet membranes, suggesting that the SW structure feature is not suitable for the FO process, consistent with findings of other studies [9,25].

Fourth, there was difference in test conditions between the two tests. In the lab-scale test, the flow rate of both sides of the solution was maintained. However, in the pilot-scale test, it was impossible to adjust the flow rate of the draw solution to that of the feed solution. This will be further discussed in the next section in detail.

### 3.2. Spiral-wound structure characteristics

Many FO tests using flat sheet FO membranes have been operated at the same flow rate for either side of solution because the flat sheet type membrane has a minimal pressure drop [21,22,24]. However, in the real field of membrane process, SWFO elements are connected to compose a multi-stage array. The draw solution is larger than the feed solution at the end of the element. As mentioned earlier, the SWFO membrane has special structure configuration compared to the flat sheet membrane. Therefore, it is necessary to identify the effects of the SWFO membrane structure characteristics on FO performance. In this section, we investigated the effect of SWFO structure

on the flow rate and pressure on either side of the solution.

With fixed flow rate of the draw solution, the feed solution flow rate was changed (Fig. 6(a) and (b)). This test method was used in other cases in the same manner (change of draw solution flow rate with a fixed feed flow rate). When we changed the feed solution flow rate, the draw solution flow rate decreased from 0.525 to 0.462 LPM (about 10% decrease, Fig. 6(a)). When we changed the draw solution flow rate, the feed solution flow rate dropped from 6.8 to 6.6 LPM (3% decrease, Fig. 6(b)). These results indicate that the feed solution flow rate changes significantly affected the draw solution flow rate. However, the effect of draw solution flow rate change was minimal. Similar results have been reported in previous studies [16,26,27]. Figs. 4 and 5 can be used to explain this result. The draw flow path is spiral, but the feed flow path is straight. The pressure drop can develop more severely on the draw side compared to that on the feed side. Therefore, the feed side solution can pressurize against the draw flow path at the end side of element.

In addition, the pressure of the feed side is always higher than that of the draw side in SWFO, preventing excess pressure on the draw side over that of the feed side (prevention of PRO mode). This feature can also pressurize the draw flow path. Due to these reasons induced by structural characteristics and operating conditions, the feed solution can significantly influence the draw solution.

We also investigated the relationship between inlet pressure and flow rate according to the type of element array. Results are shown in Fig. 6(c). In this experiment, a pump inverter controlled only one side of the flow. Tap water was used as feed solution and draw solution. Flow rate increased as the inlet pressure increased (inlet pressure was proportional with the flow rate) for both stage modes. The flow rate increased on the feed side more than on the draw side.

For example, when the inlet pressure on the feed side was adjusted to 0.2 bar, the feed flow rate was 5 LPM. However, the draw flow rate did not reach one LPM at the same inlet pressure. When the two-stage and the one-stage modes were compared to each other, the one stage mode was significantly influenced by the inlet pressure change, meaning that greater pressure drop in the two-stage mode interrupted the flow rate change through the two-stage series connection. In addition, when we applied the same inlet pressure, the two-stage mode had a decreased flow rate compared to the one-stage mode. As mentioned earlier, this result was due to a high-pressure drop on the draw side.

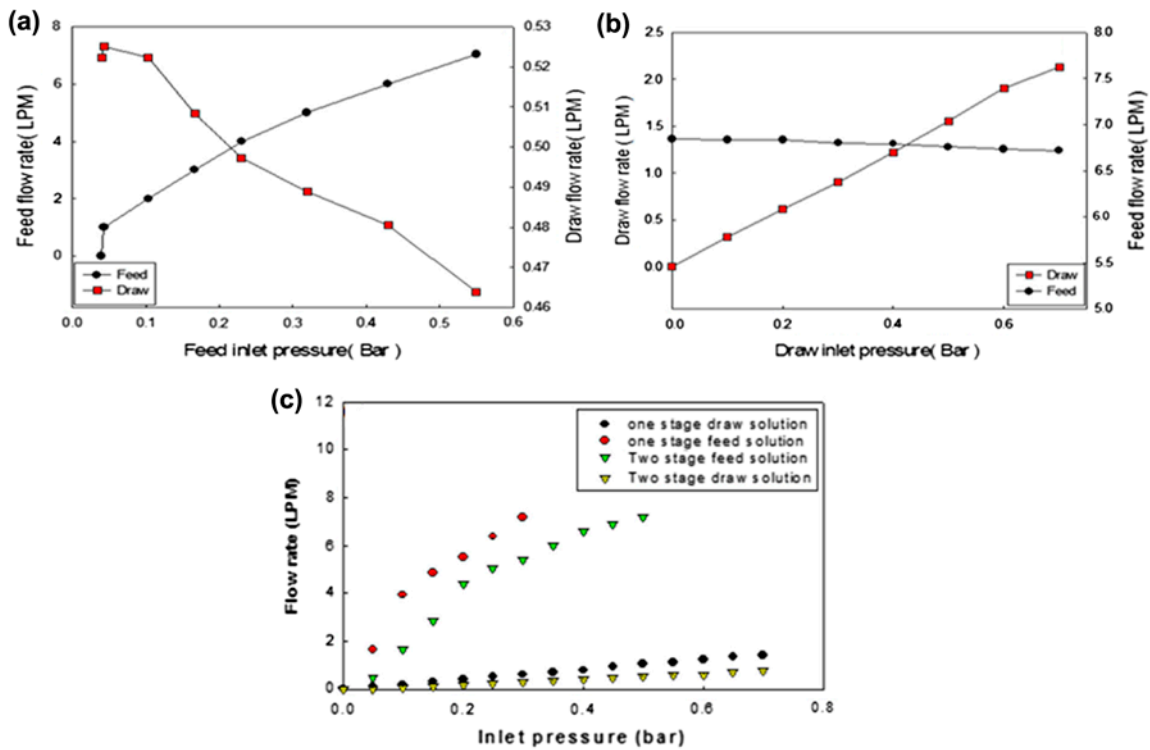


Fig. 6. Flow rate change curve of the SWFO structure (no osmotic difference between feed and draw sides of the membrane): (a) feed solution flow rate change, (b) draw solution flow rate change, and (c) comparison of the two and one-stage modes.

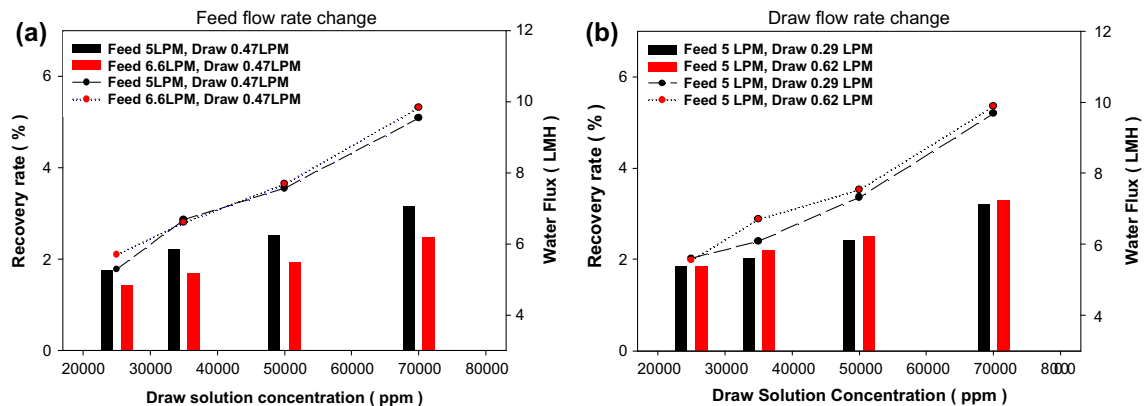


Fig. 7. Effect of feed and draw flow rates on water flux and recovery rate in the one-stage mode of the SWFO element: (a) effects of feed flow rate change (5, 6.6 LPM) when draw flow rate is fixed at 0.47 LPM, (b) effects of draw flow rate change (0.29, 0.62 LPM) when feed flow rate is fixed at 5 LPM. The pressure difference between feed inlet and draw inlet was maintained at 0.2–0.3 bar (manufacturer's recommendation). The feed inlet pressure was maintained under one bar. The draw inlet pressure was maintained under 0.7 bar. All experiments were stopped when the volume of the feed solution was half reduced.

Therefore, it was impossible to adjust the flow rate equally on both sides of the SWFO element.

In general, energy consumption and pressure in the membrane process have great correlations with

element scale and array type. In most membrane processes, multi-stack elements are used for water treatment and desalination [11,16,28]. Therefore, we need to study element scales and array types in detail.

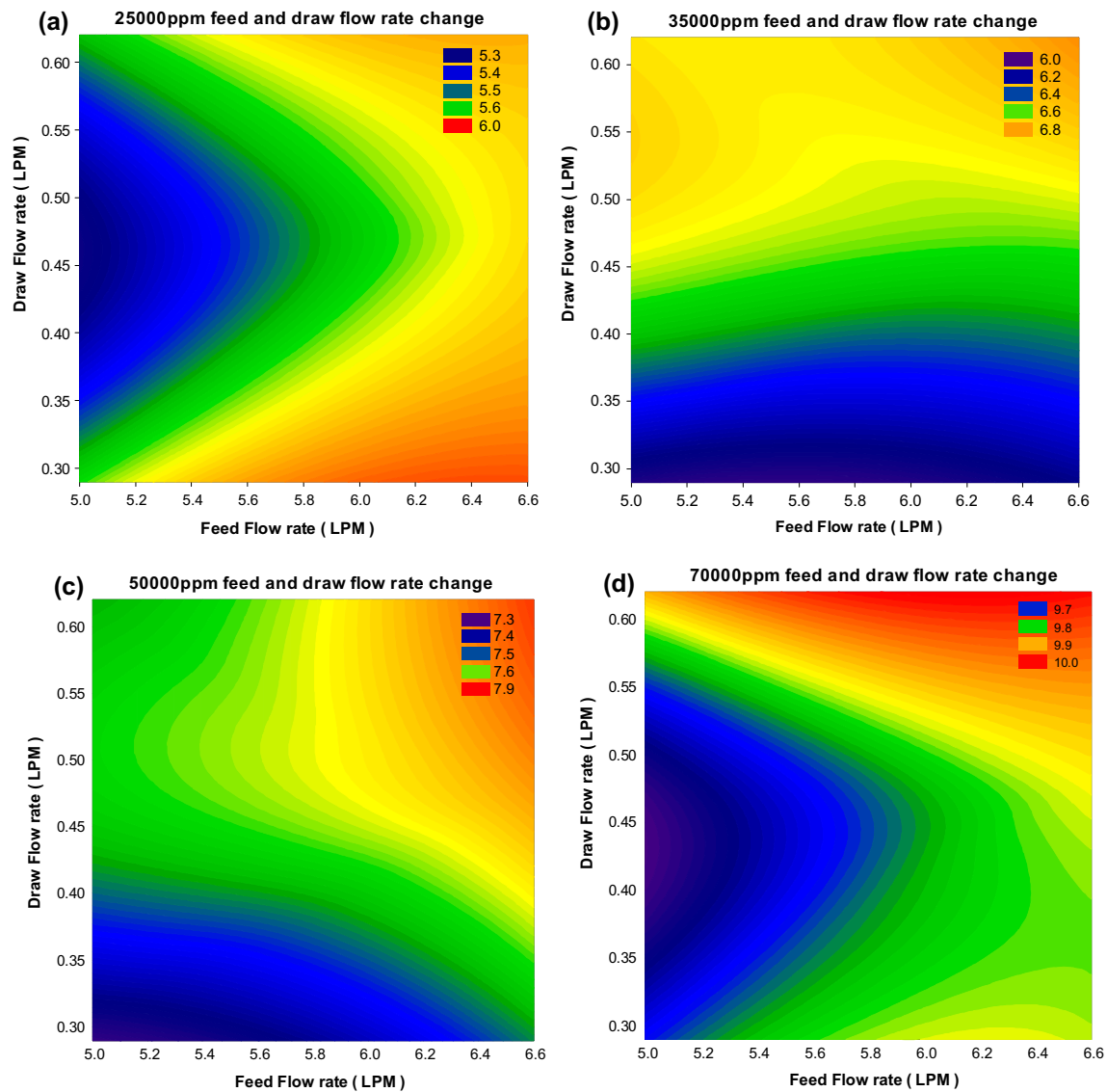


Fig. 8. Effect of the flow rate on water flux trend at varying draw solution concentrations in the one-stage mode: (a) 25,000 ppm, (b) 35,000 ppm, (c) 50,000 ppm, and (d) 70,000 ppm. Color represents mean water flux. Blue colors represent low water flux while red colors represent high water flux.

### 3.3. Impact of flow rate change on water flux and recovery rate—one-stage mode (parallel array)

Water flux has a close relationship with recovery rate. Increases in water flux and recovery rate can reduce the membrane area and the requirement for the total number of SWFO elements in real pilot plant. This means that high water flux and recovery rates can reduce CAPEX. In this study, the effect of flow rate on water flux and recovery rate in the one-stage SWFO process was evaluated at varying draw solution concentrations. The water flux and recovery rate curves are shown in Fig. 7. As shown in Fig. 7(a), the

water flux increased approximately one LMH when the feed flow rate increased from 5 to 6.6 LPM, consistent with results of previous studies [10,29,30].

Although we used DI water as feed solution, we assumed that a reverse salt diffusion could make a CECP layer on feed side. When the feed flow rate is increased, cross-flow velocity shear force can reduce the CECP layer [1,15,18]. Thus, increased feed flow rate can have a positive effect on water flux.

However, increased feed flow rate had a negative influence on the recovery rate in the performance of the one-stage SWFO membrane. The increased

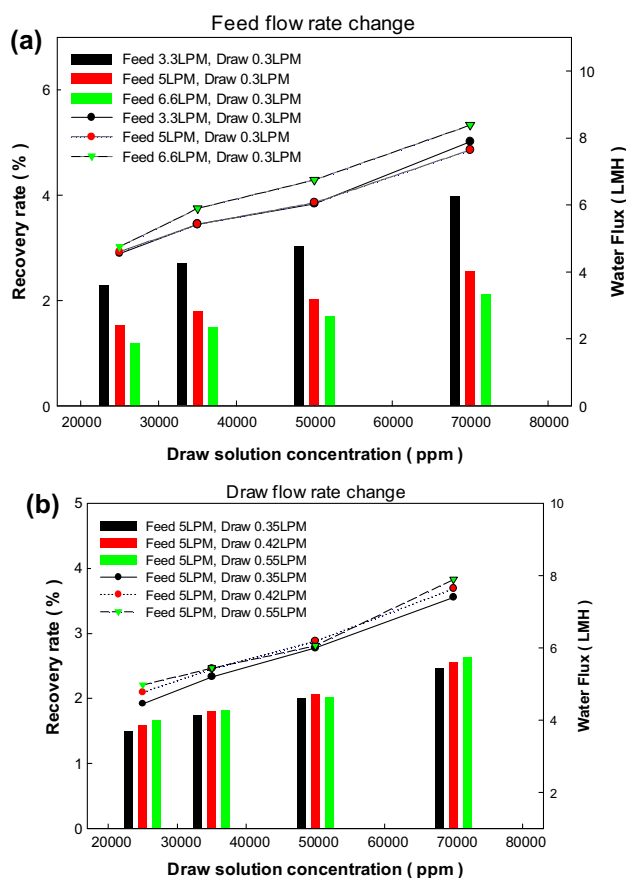


Fig. 9. Effect of feed flow rate and draw flow rate on water flux and recovery rate in the two-stage mode of the SWFO element: (a) effect of feed flow rate change (3.3, 5, 6.6 LPM) when the draw flow rate was fixed at 0.3 LPM and (b) effect of draw flow rate change (0.35, 0.42, 0.55 LPM) when the feed flow rate was fixed at five LPM. The pressure difference between the feed inlet and draw inlet was maintained at 0.2–0.3 bar (manufacturer's recommendation). The feed inlet pressure was maintained under one bar. The draw inlet pressure was maintained under 0.7 bar. All experiments were stopped when the volume of feed solution was reduced by half.

amount on the feed side flow rate was higher than the water flux rate (Eq. (3)). Therefore, the recovery rate decreased. This is why we need to optimize the feed flow rate considering both water flux and recovery rate [15,20]. As shown in Fig. 7(b), the water flux and recovery rate were also changed according to the draw flow rate. When the draw flow rate was increased, water flux increased due to reduced CP (DECP and DICP) and the dilution effect [23,31,32]. When the draw solution flow rate was changed, the recovery rate increased because the flow rate of the draw solution was not directly involved in Eq. (3). Therefore, the SWFO element test was affected by flow rate change on either side,

meaning that FO process engineers must know the element operating conditions and membrane structure, because multi-stages element are a routine configuration in FO pilot plants.

The effect of flow rate change coming from both sides on water flux at various draw solution concentrations is shown in Fig. 8. The  $x$ -axis and  $y$ -axis represent the feed solution flow rate and draw solution flow rate, respectively. Water flux changed from five to 10 LMH, in accordance with changes in draw solution concentration. At all concentrations of draw solution, it was difficult to find consistency. This phenomenon may be due to the characteristic of pilot-scale test, making it difficult to maintain test conditions during the SWFO element test.

Despite such inconsistency, we observed that each optimized point of FO performance in different concentrations generally depended on the flow rate. At a low concentration of 25,000 ppm, the feed flow rate significantly affected water flux. However, as the concentration increased to 35,000–70,000 ppm, water flux was significantly affected by the draw flow rate. As shown in Fig. 8(b), when the draw flow rate was at 0.4 LPM, the water flux was maintained at 6.5 LMH at all feed flow ranges, indicating that the feed flow rate had little influence on water flux in the one-stage mode.

### 3.4. Impact of flow rate change on water flux and recovery rate: two-stage mode (series array)

The water flux and recovery rate at varying draw concentrations with different feed and draw flow rates in the two-stage mode are shown in Fig. 9(a) and (b). These results showed a similar pattern to those in the one-stage mode. As expected, increases in both flow rate and draw solution concentration had positive effects on water flux. However, the recovery rate improved only by increased draw flow rate. Flow rate and concentration are known to have positive effects on water flux in the FO process because an increase in concentration and flow rate can cause a higher osmotic pressure difference, thus reducing the CP layer with an enhanced mass transfer coefficient [23,27].

Water flux in the two-stage mode was lower than that in the one-stage mode (parallel array). Membrane length in the two-stage mode was longer than that in the one-stage mode, causing a significant dilution effect. In the two-stage mode, two SWFO elements were connected in series (Fig. 2c), with both sides of the effluent entering the second SWFO element, indicating that the draw solution concentration of the second SWFO element was lower than that of the first SWFO element. Therefore, the osmotic pressure

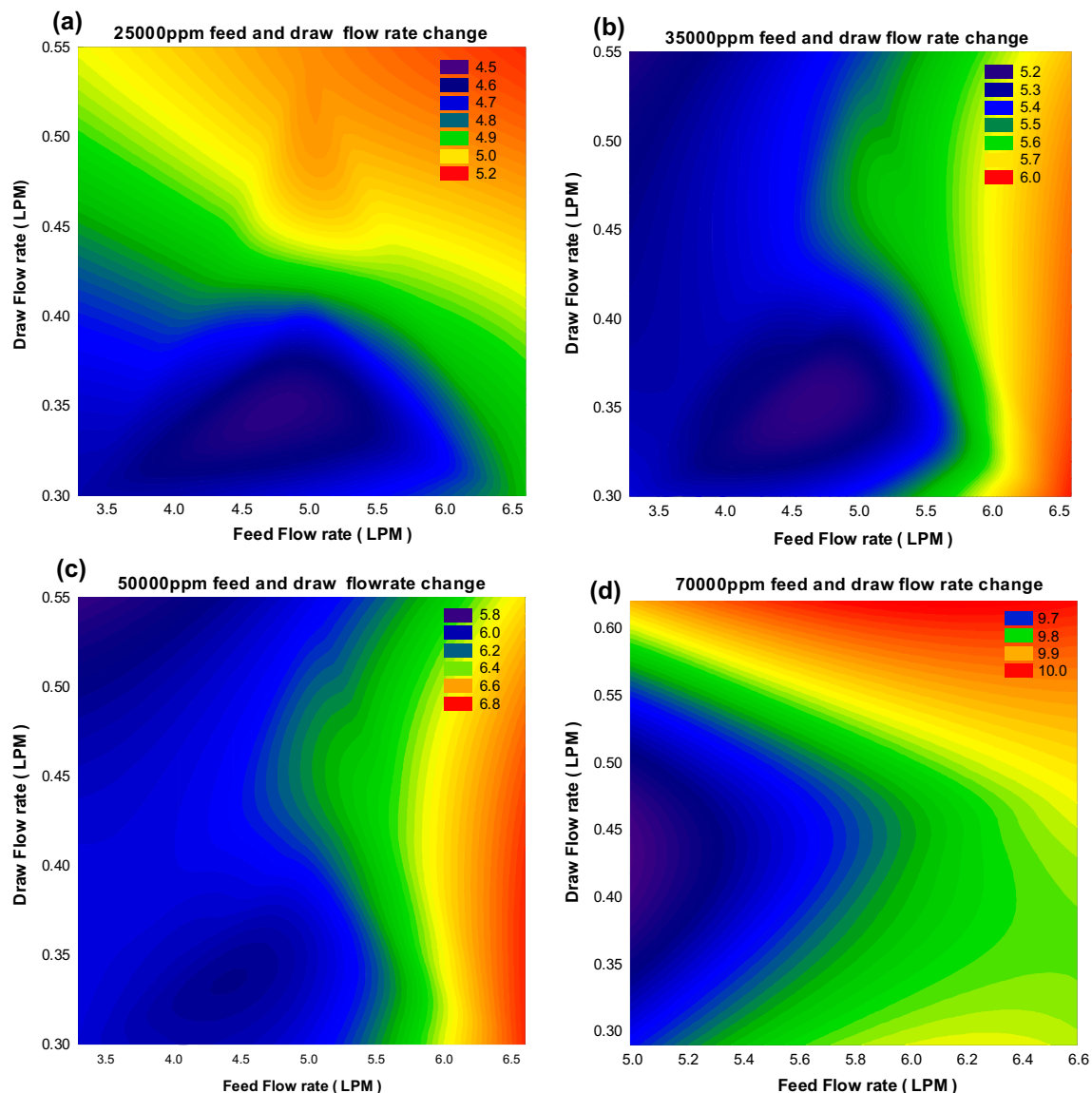


Fig. 10. Effect of flow rate on water flux trend at varying draw solution concentrations in the two-stage mode: (a) 25,000 ppm, (b) 35,000 ppm, (c) 50,000 ppm, and (d) 70,000 ppm. The color represents mean water flux. Blue colors represent low water flux. Red colors represent high water flux.

difference (driving force) decreased. The water flux trend in Fig. 9(a) and (b) showed that the flow rate increased, which might have reduced the CP layer and the dilution effect [6,9,10,13,15].

In this experiment, DI water was used as feed solution, which can result in negligible CECF. However, reverse solute diffusion inevitably occurs in the FO process, leading to the increased ionic strength of the feed solution. Therefore, alternation of feed flow rate can improve the mass transport coefficient, thus increasing the water flux.

In the one-stage mode, the recovery rate was reduced by 15–20% when the feed flow rate increased.

Thus, we estimate that the recovery rate in the two-stage mode can decrease when the feed flow rate is increased, similar to the one-stage mode. However, the ratio of the recovery rate decrease with feed flow rate change in the two-stage mode was lower than that in the one-stage mode, with a decrease of approximately 30%. As mentioned above, water flux in the two-stage mode was lower than that in the one-stage mode due to the fact that recovery rate could be affected by the dilution effect and permeate flow rate (Eq. (3)).

In addition, the fixed draw flow rate was different in the two tests. In the one-stage mode, the draw flow

rate was 0.47 LPM. In the two-stage mode, the draw flow rate was 0.3 LPM. The lower water flux was attributed to draw flow rate (Fig. 6). Therefore, in the process using the SWFO element, flow rate can significantly affect pressure drop, water flux, recovery rate, dilution effect, and CP.

We further studied the flow rate effects in the SWFO element test by comparing water flux as a function of the feed/draw flow rate and draw solution concentration (Fig. 10) [13,24,27,33]. Across all draw solution concentrations, water flux was generally low under the conditions of low feed rate and draw flow rate. In both tests, the effect of the draw flow rate on water flux was more obvious compared to feed flow rate because the dilution effect was minimum with a low water flux. In contrast, as the draw concentration increased, the water flux was more dependent on feed solution than draw solution (Fig. 10(b), (c), and (d)).

In addition, the membrane support layer is an unstirred layer unaffected by flow rate or reduced DICP [15,17]. However, in this study, ionic strength in feed solution was found to be an important factor for water flux, which is in agreement with previous reports [2,11]. Although DI water was used as feed water, the ionic strength increased with RSF. This test lasted until concentration rate reached two ionic strengths of nearly 3 mS/cm at the end of the test. RSF was increased as a function of concentration gradient [23,34]. Thus, it is expected that the RSF will increase when the draw solution concentration increases [23,34].

In element scale SWFO test, the water flux and RSF significantly diluted the draw solution, resulting in concentrated feed solution. High RSF at a high draw solution concentration might have caused CECP on the membrane surface layer. The feed flow rate might have affected the removal of the CECP layer. In the two-stage mode, both sides of solution stayed inside the element longer than in the one-stage mode. Therefore, the ionic strength of the feed side significantly increased. Consequently, the increase in flow rate of the feed solution affected water flux at high draw concentrations.

#### 4. Conclusions

In this study, we found that the results from a lab-scale test could not be directly applied in a pilot-scale plant. The effect of element structural characteristics, array, and flow rate on SWFO performance was determined. We summarized the results as follow:

- (1) A spiral-wound element is different from a flat sheet membrane in structural configuration, causing a significant pressure drop due to its draw flow path, which was longer and more tightly wound than the feed flow path. In addition, the effective membrane area was reduced due to formation of dead zone area.
- (2) The increased flow rates on both sides of the membrane had a positive effect on the membrane surface by increasing shear forces (mass transfer coefficient), thus reducing the effect of dilution CP.
- (3) Based on the results of our tests according to the types of array (one- and two-stage modes), solution retention time was different due to SWFO structural characteristics. In the two-stage mode, a long retention time and increased ionic strength significantly affected FO performance, which was why the feed flow rate affected water flux more than the draw flow rate.

Therefore, before commercialization, a pilot-scale test regarding operating conditions such as draw solution concentration, flow rate, and the type of element array, must be conducted.

#### Acknowledgments

This research was supported in part by a grant (code 15IFIP-B088091-02) from the Industrial Facilities and Infrastructure Research Program funded by Ministry of Land, Infrastructure and Transport of the Korean government. This research was also supported in part by the Korean Ministry of Environment (MOE), as a Knowledge-based environmental service (Waste to energy recycling, Eco design) and the Human resource development Project.

#### References

- [1] Q. Yang, K.Y. Wang, T.-S. Chung, Dual-layer hollow fibers with enhanced flux as novel forward osmosis membranes for water production, *Environ. Sci. Technol.* 43 (2009) 2800–2805.
- [2] G. Blandin, A.R.D. Verliefde, C.Y. Tang, P. Le-Clech, Opportunities to reach economic sustainability in forward osmosis–reverse osmosis hybrids for seawater desalination, *Desalination* 363 (2015) 26–36.
- [3] L.F. Greenlee, D.F. Lawler, B.D. Freeman, B. Marrot, P. Moulin, Reverse osmosis desalination: Water sources, technology, and today's challenges, *Water Res.* 43 (2009) 2317–2348.
- [4] R. Semiat, Energy issues in desalination processes, *Environ. Sci. Technol.* 42 (2008) 8193–8201.

- [5] C. Fritzmann, J. Löwenberg, T. Wintgens, T. Melin, State-of-the-art of reverse osmosis desalination, *Desalination* 216 (2007) 1–76.
- [6] S. Chakraborty, M. Pal, M. Roy, P. Pal, Water treatment in a new flux-enhancing, continuous forward osmosis design: Transport modelling and economic evaluation towards scale up, *Desalination* 365 (2015) 329–342.
- [7] R. Valladares Linares, Z. Li, M. Abu-Ghdaib, C.-H. Wei, G. Amy, J.S. Vrouwenvelder, Water harvesting from municipal wastewater via osmotic gradient: An evaluation of process performance, *J. Membr. Sci.* 447 (2013) 50–56.
- [8] T. Cath, A. Childress, M. Elimelech, Forward osmosis: Principles, applications, and recent developments, *J. Membr. Sci.* 281 (2006) 70–87.
- [9] D. Attarde, M. Jain, K. Chaudhary, S.K. Gupta, Osmotically driven membrane processes by using a spiral wound module—Modeling, experimentation and numerical parameter estimation, *Desalination* 361 (2015) 81–94.
- [10] Y.C. Kim, S.J. Park, Experimental study of a 4040 spiral-wound forward-osmosis membrane module, *Environ. Sci. Technol.* 45 (2011) 7737–7745.
- [11] N.T. Hancock, P. Xu, M.J. Roby, J.D. Gomez, T.Y. Cath, Towards direct potable reuse with forward osmosis: Technical assessment of long-term process performance at the pilot scale, *J. Membr. Sci.* 445 (2013) 34–46.
- [12] Y. Sato, S.-I. Nakao, Theoretical estimation of semi-permeable membranes leading to development of forward osmosis membranes and processes as a future seawater desalination technology, *Desalin. Water Treat.* 57(12) (2016) 5398–5405.
- [13] A. Achilli, T.Y. Cath, A.E. Childress, Selection of inorganic-based draw solutions for forward osmosis applications, *J. Membr. Sci.* 364 (2010) 233–241.
- [14] E. Nagy, A general, resistance-in-series, salt- and water flux models for forward osmosis and pressure-retarded osmosis for energy generation, *J. Membr. Sci.* 460 (2014) 71–81.
- [15] J.E. Kim, S. Phuntsho, F. Lotfi, H.K. Shon, Investigation of pilot-scale 8040 FO membrane module under different operating conditions for brackish water desalination, *Desalin. Water Treat.* 53 (2014) 2782–2791.
- [16] J. Schwinge, P.R. Neal, D.E. Wiley, D.F. Fletcher, A.G. Fane, Spiral wound modules and spacers, *J. Membr. Sci.* 242 (2004) 129–153.
- [17] J. Fárková, The pressure drop in membrane module with spacers, *J. Membr. Sci.* 64 (1991) 103–111.
- [18] S. Sundaramoorthy, G. Srinivasan, D.V.R. Murthy, An analytical model for spiral wound reverse osmosis membrane modules: Part I—Model development and parameter estimation, *Desalination* 280 (2011) 403–411.
- [19] A. Da Costa, A. Fane, D. Wiley, Spacer characterization and pressure drop modelling in spacer-filled channels for ultrafiltration, *J. Membr. Sci.* 87 (1994) 79–98.
- [20] Z. Cao, D. Wiley, A. Fane, CFD simulations of net-type turbulence promoters in a narrow channel, *J. Membr. Sci.* 185 (2001) 157–176.
- [21] M. Shibuya, M. Yasukawa, T. Takahashi, T. Miyoshi, M. Higa, H. Matsuyama, Effect of operating conditions on osmotic-driven membrane performances of cellulose triacetate forward osmosis hollow fiber membrane, *Desalination* 362 (2015) 34–42.
- [22] C. Kim, S. Lee, S. Hong, Application of osmotic backwashing in forward osmosis: Mechanisms and factors involved, *Desalin. Water Treat.* 43 (2012) 314–322.
- [23] W.A. Phillip, J.S. Yong, M. Elimelech, Reverse draw solute permeation in forward osmosis: Modeling and experiments, *Environ. Sci. Technol.* 44 (2010) 5170–5176.
- [24] B. Gu, D.Y. Kim, J.H. Kim, D.R. Yang, Mathematical model of flat sheet membrane modules for FO process: Plate-and-frame module and spiral-wound module, *J. Membr. Sci.* 379 (2011) 403–415.
- [25] M. Kostoglou, A. Karabelas, On the fluid mechanics of spiral-wound membrane modules, *Ind. Eng. Chem. Res.* 48 (2009) 10025–10036.
- [26] Y. Xu, X. Peng, C.Y. Tang, Q.S. Fu, S. Nie, Effect of draw solution concentration and operating conditions on forward osmosis and pressure retarded osmosis performance in a spiral wound module, *J. Membr. Sci.* 348 (2010) 298–309.
- [27] G. Schock, A. Miquel, Mass transfer and pressure loss in spiral wound modules, *Desalination* 64 (1987) 339–352.
- [28] S. Lim, H. Park, H. Lee, K. Yum, H. Lee, D. Woo, Application of seawater dilution process to SWRO filtration system for low-energy desalination, *Desalin. Water Treat.* 57(16) (2016) 7414–7421.
- [29] A. Achilli, T.Y. Cath, A.E. Childress, Power generation with pressure retarded osmosis: An experimental and theoretical investigation, *J. Membr. Sci.* 343 (2009) 42–52.
- [30] T.Y. Cath, Osmotically and thermally driven membrane processes for enhancement of water recovery in desalination processes, *Desalin. Water Treat.* 15 (2012) 279–286.
- [31] A. Sagiv, A. Zhu, P.D. Christofides, Y. Cohen, R. Semiat, Analysis of forward osmosis desalination via two-dimensional FEM model, *J. Membr. Sci.* 464 (2014) 161–172.
- [32] S. Lee, Y.C. Kim, S.-J. Park, S.-K. Lee, H.-C. Choi, Experiment and modeling for performance of a spiral-wound pressure-retarded osmosis membrane module, *Desalin. Water Treat.* 57(22) (2016) 10101–10110.
- [33] Y. Kim, J.H. Lee, Y.C. Kim, K.H. Lee, I.S. Park, S.-J. Park, Operation and simulation of pilot-scale forward osmosis desalination with ammonium bicarbonate, *Chem. Eng. Res. Des.* 94 (2015) 390–395.
- [34] N.T. Hancock, T.Y. Cath, Solute coupled diffusion in osmotically driven membrane processes, *Environ. Sci. Technol.* 43 (2009) 6769–6775.